Continental margin molybdenum isotope signatures from the early Eocene

Alexander J. Dickson [*],[1], Anthony S. Cohen, Angela L. Coe

Department of Environment, Earth and Ecosystems, The Open University, Walton Hall, Milton Keynes, MK7 6AA, UK

A B S T R A C T

Molybdenum (Mo) isotope compositions of marine sedimentary deposits that span the Paleocene–Eocene Thermal Maximum (PETM, approximately 56 Ma) are presented from two Tethys Ocean sites (Guru Fatima, Tajikistan and Kheu River, Georgia). Local redox indicators suggest that both locations experienced anoxia and intervals of euxinia (with hydrogen sulphide present in seawater) during the early part of the PETM. However, the Mo-isotope compositions (expressed as $\delta^{98/95}$Mo) for each site differ significantly. Local redox conditions were very stable at Guru Fatima, where $\delta^{98/95}$Mo reached a maximum of 0.96‰, which is ~0.7‰ lower than for early Eocene seawater as recently inferred from euxinic Arctic Ocean deposits. This observation supports the argument that a ~0.7‰ difference between seawater and anoxic continental margin marine sediments documented at the present day might also be found in the paleo-record. In contrast, local redox conditions at Kheu River were not stable over the study interval, and $\delta^{98/95}$Mo were much lower than at Guru Fatima. The low $\delta^{98/95}$Mo values at Kheu River are attributed to the influence of post-depositional remobilization of Mo by repeated adsorption and dissolution of Fe–Mn oxides during brief intervals of bottom water oxidation. The data highlight the importance of obtaining multi-proxy constraints on both local redox and paleoceanographic setting before the Mo-isotope compositions of sedimentary deposits can be interpreted accurately.

© 2014 Elsevier B.V. All rights reserved.

1. Introduction

Over recent years there has been significant interest in understanding the role of seawater oxygen concentrations in driving and responding to ecological and environmental change, both past and present. This interest has led to the development of several geochemical proxies to constrain the oxygenation state of seawater using marine sedimentary deposits. These techniques include redox sensitive trace element enrichments (Emerson and Huested, 1991; Crusius et al., 1996; Tribovillard et al., 2006), proportions of reactive and unreactive iron species (e.g. Raiswell et al., 1988; Canfield, 1989), organic biomarkers (Summons and Powell, 1987; Pancost et al., 2004) and variations in the stable isotope compositions of redox sensitive elements such as molybdenum, uranium and chromium (e.g. Siebert et al., 2003; Stirling et al., 2007; Pearce et al., 2008; Weyer et al., 2008; Montoya-Pino et al., 2010; Brennecka et al., 2011). In particular, trace metal abundances have proven to be useful indicators of marine redox conditions. Variations in sedimentary trace metal abundances can result from the changing solubility of elements as their oxidation states alter, and/or variable speciation under differing levels of dissolved oxygen in seawater and in sediment pore waters (Tribovillard et al., 2006; Piper and Calvert, 2009). Enrichments of trace elements alone, however, can be strongly overprinted by changes in the dissolved trace metal inventory in seawater either due to expansion/contractions in the extent of marine anoxia globally, or within hydrographically restricted basins (Algeo and Lyons, 2006). For these reasons, the redox dependency of the isotope compositions of transition metal elements (including molybdenum, uranium, chromium) has recently been explored as redox proxies to circumvent 'reservoir' effects on trace metal inventories and to obtain better estimates of marine redox conditions over a range of spatial scales.

The molybdenum (Mo) isotope composition of marine sedimentary deposits (expressed as $\delta^{98/95}\text{Mo} = ((^{98/95}\text{Mo}_{sample} - {}^{98/95}\text{Mo}_{standard})/{}^{98/95}\text{Mo}_{standard}) * 1000)$ has been particularly useful as a seawater redox proxy, because Mo removal from seawater carries distinct isotope fractionations that depend upon the local redox environment (Fig. 1). The global balance of the redox-dependent Mo fluxes determines the isotopic composition of seawater (e.g. Siebert et al., 2003; Poulson-Brucker et al., 2009).

* Corresponding author.
  E-mail address: alex.dickson@earth.ox.ac.uk (A.J. Dickson).
[1] Preset address: Department of Earth Sciences, University of Oxford, South Parks Road, Oxford, OX1 3AN, UK.
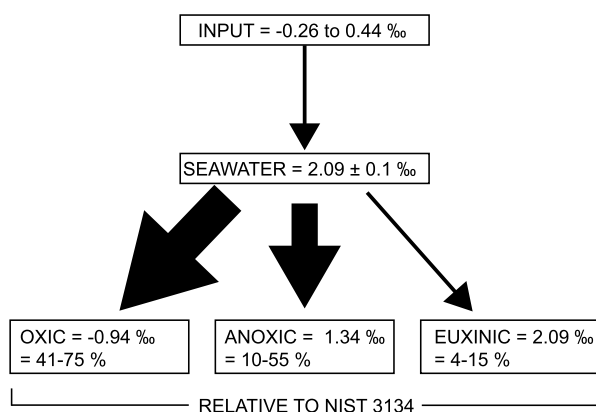
Fig. 1. Global Mo fluxes calculated using $\delta^{98/95}$Mo data from different laboratories (Siebert et al., 2003; Poulson et al., 2006; Poulson-Brucker et al., 2009; Archer and Vance, 2008; Neubert et al., 2008; Greber et al., 2012; Goldberg et al., 2013) renormalised to NIST 3134 (Goldberg et al., 2013). The range of the euxinic, anoxic and oxic Mo fluxes are determined by the choice of $\delta^{98/95}$Mo for riverine input (igneous rocks $= -0.26‰$, Siebert et al., 2003 or mean river water $= 0.44‰$, Archer and Vance, 2008), and by varying the size of the euxinic flux according to divergent past estimates ($<5\%$, Neubert et al., 2008 versus $\sim15\%$, Scott et al., 2008). Estimates are largely within the uncertainties of previous mass balances for Mo (Morford and Emerson, 1991; Poulson-Brucker et al., 2009).

Mo-isotope compositions of past seawater have been inferred from measurements of sedimentary deposits from euxinic environments (e.g. Arnold et al., 2004; Lehmann et al., 2007; Pearce et al., 2008; Wille et al., 2008; Gordon et al., 2009; Wen et al., 2009; Duan et al., 2010; Kendall et al., 2011; Dickson et al., 2012; Dickson and Cohen, 2012; Zhou et al., 2012) under the assumption that in highly sulphidic conditions ('euxinic,' with >11 μmol/l H_2S, Eriksson and Helz, 2000; Neubert et al., 2008), Mo is removed quantitatively from seawater into seafloor sediments. In these instances, the possible confounding influence of variable isotope fractionations imparted by non-quantitative Mo scavenging by sedimentary phases such Fe and Mn-oxides (Goldberg et al., 2009; Barling and Anbar, 2004; Siebert et al., 2003), and by conversion of Mo to thiomolybdates ($MoO_xS_{4-x}^{2-}$) under low-sulphide concentrations (e.g. Tossell, 2005; Eriksson and Helz, 2000; Nägler et al., 2011) are, theoretically, avoided.

A key question regarding the interpretation of Mo-isotope systematics at the present day is the origin of a $\sim0.7‰$ offset observed between sediments deposited in anoxic open-ocean (continental margin) settings and coeval seawater ($\Delta Mo = \delta^{98/95}Mo_{seawater} - \delta^{98/95}Mo_{anoxic\,sediments}$) (Poulson et al., 2006; Poulson-Brucker et al., 2009). This fractionation, which has been used to calculate the present-day fluxes of Mo into different marine redox environments (Poulson-Brucker et al., 2009, recalculated in Fig. 1), may either reflect a mechanism of Mo incorporation into anoxic sediments by conversion to sulphide (e.g. Poulson et al., 2006; Siebert et al., 2006; Poulson-Brucker et al., 2012) or a fortuitous mixing of Mo-isotope fractionations imparted by conversion to $MoO_xS_{4-x}^{2-}$, and by adsorption to organic matter/pyrite and Fe/Mn-oxides (Barling and Anbar, 2004; Goldberg et al., 2009; Poulson-Brucker et al., 2012). Reproduction of the $\Delta0.7‰$ offset in the paleo-record would support the former mechanism, but this has not previously been demonstrated.

A second key question is the extent to which Mo-isotope compositions in organic-rich sediments record the Mo-isotope composition of coeval seawater. Independent evidence is required to verify the presence of highly sulphidic depositional conditions (with $H_2S > 11$ μmol/l, Neubert et al., 2008) that are required for sedimentary Mo-isotope compositions to approach the seawater value (e.g. Poulson et al., 2006; Gordon et al., 2009). To date, however, there is no proxy that can be used to quantitatively reconstruct the concentration of H_2S in past seawater, despite

some preliminary efforts (e.g. Arnold et al., 2012). Furthermore, there is evidence that Mo can be remobilised if redox conditions in the sediment change after deposition (e.g. Reitz et al., 2007; Scheiderich et al., 2010), thus altering the primary Mo-isotope composition and limiting the use of Mo-isotopes to reconstruct primary depositional processes (e.g. Siebert et al., 2006; Poulson et al., 2006).

In this paper, Mo-isotope compositions of sedimentary deposits are presented from two stratigraphic succession from the Tethys Ocean continental margin that span the Paleocene–Eocene Thermal Maximum (PETM, 56 Myr ago). The main aim of the study is to test whether the 0.7‰ Mo-isotopic difference observed between anoxic continental margin sediments and seawater at the present day (Poulson et al., 2006; Poulson-Brucker et al., 2009) occurred during earlier intervals in Earth's history. Key to testing this hypothesis is the recent characterisation of the Mo-isotope composition of early Eocene seawater from Arctic Ocean sediments (Dickson et al., 2012; Dickson and Cohen, 2012). A secondary aim was to investigate whether slight differences in depositional conditions during the study interval (Dickson et al., 2014) caused different Mo-isotope compositions in contemporaneous sedimentary records.

2. Methods

Samples were obtained from two sections spanning the PETM at Guru Fatima, Tajikistan and Kheu River, Georgia. The geological setting of these sites has been discussed by Gavrilov et al. (1992, 1997, 2009).

$\delta^{98/95}$Mo compositions were determined under trace-metal clean laboratory conditions. Sample powders were accurately weighed and digested using inverse aqua-regia following addition of a ^{97}Mo and ^{100}Mo enriched isotope spike. Mo was purified from matrix elements and potential interferences using a single anion-exchange column pass procedure (Pearce et al., 2009) that has been shown to produce $\delta^{98/95}$Mo compositions for standard reference materials that are indistinguishable, within the ascribed uncertainties, to results from other laboratories currently producing Mo-isotope data (Goldberg et al., 2013). Analyses were made on a Thermo-Finnegan Neptune MC-ICP-MS, using solutions containing ~50 ppb natural Mo, monitoring within runs for possible interferes from Ru (^{99}Ru) and Zr (^{91}Zr). Data reduction was carried out off-line using a spreadsheet-based deconvolution routine (Pearce et al., 2009). Procedural blanks for Mo were less than ~2 ng, contributing an insignificant amount to the measured Mo. All $\delta^{98/95}$Mo data have been calculated relative to an in-house Mo solution standard (Fisher Chemicals, ICP Mo standard solution, lot 9920914-150) and have been re-normalised to NIST 3134 following Greber et al. (2012) and Goldberg et al. (2013). Data are quoted in the text relative to NIST 3134. External reproducibility for $\delta^{98/95}$Mo was $\pm0.10‰$ (2 S.D., $n = 9$), as determined by repeated processing an in-house mudrock standard (Monterey Formation sample 00N118) through the full chemical procedure. Two powder aliquots of three samples each from Guru Fatima and Kheu River were also passed through the full chemical procedure and gave indistinguishable $\delta^{98/95}$Mo values (within analytical uncertainty). Mo abundances were calculated using isotope dilution from the ^{100}Mo/^{95}Mo ratio obtained during Mo-isotope analyses. All data are listed in Tables 1 and 2.

3. Results

The new $\delta^{98/95}$Mo data are presented in Fig. 2, together with previously published geochemical data for Guru Fatima and Kheu River (Dickson et al., 2014). $\delta^{98/95}$Mo for samples from Guru Fatima exhibit a clear stratigraphic trend across the carbon isotope

Table 1
Guru-Fatima data.

Sample	Relative height (m)	$\delta^{98/95}$Mo (‰)$_{OU}$	2 S.E. uncertainty (‰)	$\delta^{98/95}$Mo (‰)$_{NIST\,3134}$[a]	2 S.E. uncertainty (‰)	[Mo] (ppm)
404	−2.7	1.01	0.03	0.64	0.05	5.64
405	−1.7	1.11	0.03	0.74	0.05	10.12
406	0	0.85	0.03	0.48	0.05	33.60
406	*0*	*0.85*	*0.05*	*0.48*	*0.06*	
407 up	0.3	1.32	0.03	0.95	0.05	949.90
407 up	*0.3*	*1.36*	*0.04*	*0.99*	*0.06*	
407 down	0.3	1.31	0.06	0.94	0.08	1113.52
407a	0.6	1.26	0.03	0.89	0.05	126.64
407a	*0.6*	*1.25*	*0.03*	*0.88*	*0.05*	
407b	1	1.09	0.03	0.72	0.05	15.86
408	1.55	0.96	0.03	0.59	0.05	11.75
409	2.55	−0.43	0.03	−0.80	0.05	1.76
410	3.45	−0.08	0.03	−0.45	0.05	1.02
411	4.5	−0.17	0.04	−0.54	0.05	0.62

[a] $\delta^{98/95}$Mo$_{[NIST]}$ calculated by subtracting 0.37‰ and propagating the uncertainties from individual analyses and the uncertainty (±0.04‰) associated with defining the difference between NIST 3134 and the OU Fisher Chemicals in-house Mo standard (Goldberg et al., 2013).

Table 2
Kheu River data.

Sample	Relative height (m)	$\delta^{98/95}$Mo (‰)	2 S.E. uncertainty (‰)	$\delta^{98/95}$Mo (‰)$_{NIST\,3134}$[a]	2 S.E. uncertainty (‰)	[Mo] (ppm)
727.000	2.68	−0.45	0.06	−0.82	0.07	0.10
724.000	2.23	−0.92	0.05	−1.29	0.07	0.21
722a	1.78	−1.59	0.06	−1.96	0.07	0.56
717.000	1.03	−0.48	0.05	−0.85	0.06	0.99
716.000	0.88	−1.23	0.05	−1.61	0.07	0.54
715.000	0.73	−1.61	0.03	−1.98	0.05	2.03
715.000	*0.73*	*−1.52*	*0.05*	*−1.89*	*0.07*	*2.18*
E4 top (top)	0.57	−0.70	0.05	−1.07	0.06	2.99
D4 top	0.48	−0.45	0.03	−0.82	0.05	9.71
D2 base	0.39	−1.08	0.05	−1.45	0.06	11.93
D1 dark top	0.37	−1.14	0.02	−1.51	0.05	12.22
C1	0.24	−0.87	0.03	−1.24	0.05	4.86
A1 8–9 cm	0.08	−0.22	0.04	−0.59	0.05	10.58
A1 8–9 cm	*0.08*	*−0.25*	*0.04*	*−0.62*	*0.06*	*10.33*
A1 6–6.5 cm	0.06	0.01	0.03	−0.36	0.05	79.33
A1 4–6 cm (bottom)	0.04	−0.27	0.03	−0.64	0.05	95.99
A1 3.5–4 cm	0.04	−0.31	0.04	−0.68	0.05	104.25
A1 1.5–3 cm (upper)	0.02	−0.39	0.04	−0.76	0.06	99.80
A1a	0.00	−0.38	0.04	−0.75	0.06	23.18
713.000	−0.15	−1.33	0.03	−1.70	0.05	1.05
713.000	*−0.15*	*−1.28*	*0.05*	*−1.65*	*0.07*	*1.03*
712.000	−0.30	−0.68	0.05	−1.05	0.06	0.57
710.000	−0.60	−1.23	0.05	−1.60	0.07	0.22
709.000	−0.75	−1.72	0.06	−2.09	0.07	0.21
707.000	−1.05	0.04	0.07	−0.33	0.08	0.07
704.000	−1.50	−0.36	0.08	−0.74	0.09	0.06
701.000	−1.95	−1.08	0.14	−1.45	0.14	0.05

[a] $\delta^{98/95}$Mo$_{[NIST]}$ calculated by subtracting 0.37‰ and propagating the uncertainties from individual analyses and the uncertainty (±0.04‰) associated with defining the difference between NIST 3134 and the OU Fisher Chemicals in-house Mo standard (Goldberg et al., 2013).

excursion (CIE) that defines the PETM. Below the CIE, $\delta^{98/95}$Mo is approximately constant at ∼0.62‰. Within the CIE $\delta^{98/95}$Mo increases to 0.99‰ and then decreases slightly up-section. Above the CIE, $\delta^{98/95}$Mo returns to lower values and averages −0.60‰.

At Kheu River, $\delta^{98/95}$Mo values oscillate between −2.01‰ and −0.33‰ throughout the section and do not show any systematic relationship with the CIE. Within the CIE, in an interval characterised by [Mo] of 5–100 ppm, i.e. significantly elevated above detrital levels (e.g. Rudnick and Gao, 2003), $\delta^{98/95}$Mo reaches maximum values of −0.36‰ and −0.82‰. These maximum values correlate approximately with maxima in Fe_{HR}/Fe_T (Fig. 2).

4. Mo-isotope evidence for Mo incorporation into Tethys Ocean sedimentary deposits

At low concentrations of H_2S (<11 µmol/l), Mo is incorporated into sediments either by adsorption onto Mn/Fe-oxides or by conversion of dissolved Mo to tetra-thiomolybdate, through a series of $MoO_xS_{4-x}^{2-}$ species (Tossell, 2005; Neubert et al., 2008; Nägler et al., 2011). The balance of these mechanisms will vary depending on whether bottom water and pore water oxygen concentrations are sufficiently high to stabilise the formation of oxide minerals. Scott and Lyons (2012) defined a model for interpreting primary redox environments from the $\delta^{98/95}$Mo of organic-carbon rich mudrock deposits. In their model, incorporation of Mo into sediments would take place by one of three processes dictated by local redox conditions: (i) fully oxic: incorporation mainly by adsorption to Mn-oxides; little Mo enrichment below sediment–water interface; (ii) weakly sulphidic: incorporation of Mo mainly by adsorption to Mn-oxides, subsequent release of Mo during Mn-oxide dissolution in porewaters, re-fixation of Mo as $MoO_xS_{4-x}^{2-}$ in the sub-surface sulphate reduction zone; typical Mo abundances range from 2 to 25 ppm; (iii) highly sulphidic: incorporation of Mo mainly by conversion to $MoO_xS_{4-x}^{2-}$; typical Mo
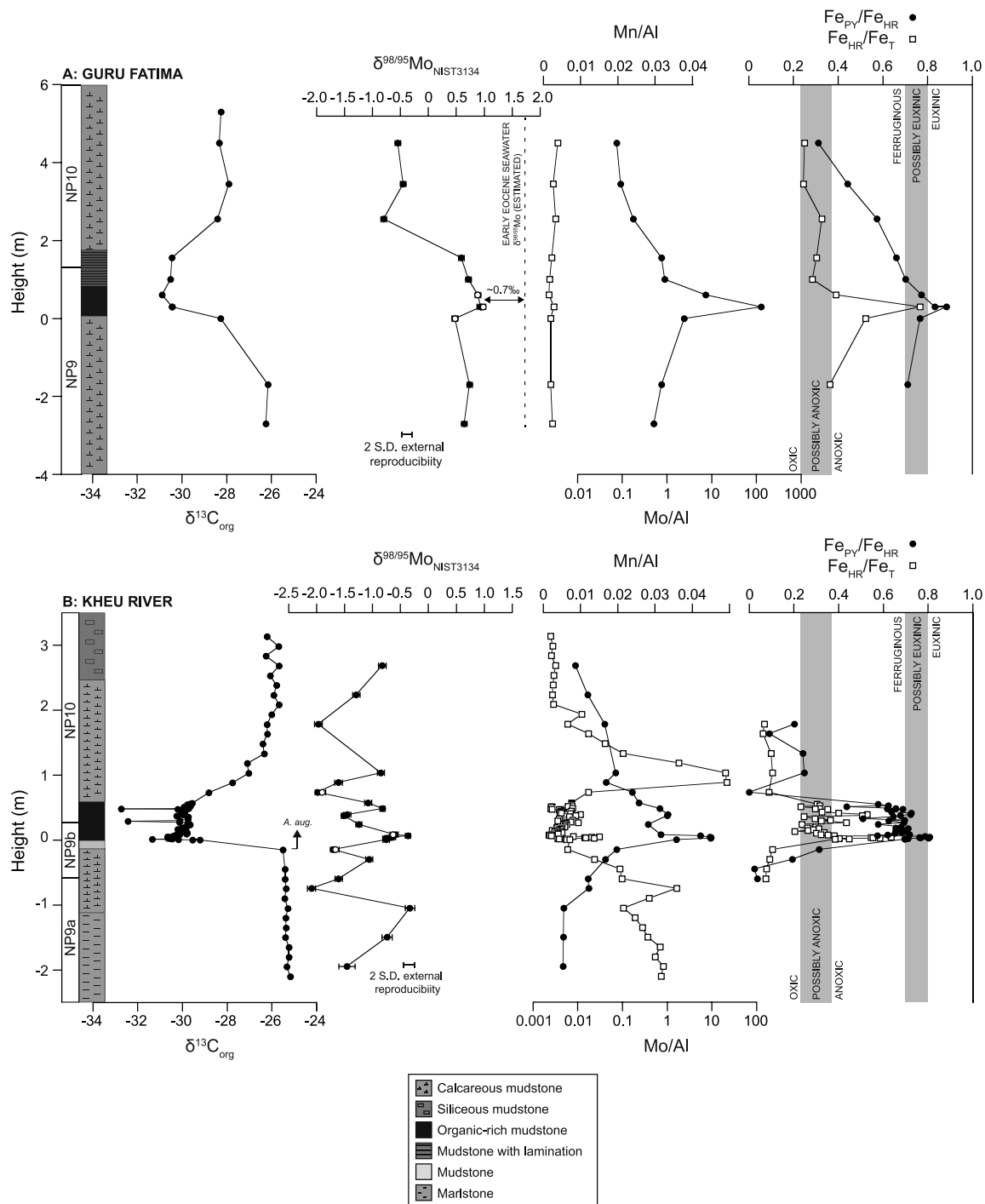
Fig. 2. Mo-isotope data for A: Guru Fatima and B: Kheu River. C-isotope, elemental abundance, and Fe-speciation data are from Dickson et al. (2014).

abundances >100 ppm. Importantly, these three processes will produce distinct $\delta^{98/95}$Mo compositions, since adsorption of dissolved Mo- to Mn-oxides carries a large ($-3\permil$) isotope fractionation (Siebert et al., 2003; Barling and Anbar, 2004), while conversion to $MoO_xS_{4-x}^{2-}$, under progressively higher dissolved H_2S concentrations, promotes the incorporation into sediments of Mo with a $\delta^{98/95}$Mo closer to seawater (e.g. McManus et al., 2002; Siebert et al., 2006; Poulson et al., 2006; Reitz et al., 2007; Scott and Lyons, 2012).

Bottom water oxygen concentrations at Guru Fatima were low and relatively constant during sediment deposition. Stability of the redox-cline is indicated by an invariant Mn/Al ratio that ap-

proximates the average continental crust value (Rudnick and Gao, 2003) and argues against the cycling of Mn-oxides across the sediment–water interface (Dickson et al., 2014). In accord with inferences from local redox indicators, $\delta^{98/95}$Mo are uniformly higher at Guru Fatima than at Kheu River, and preserve a stratigraphic trend of $\delta^{98/95}$Mo that correlates with the negative CIE (Fig. 2). The absence of Mn-oxide fixation makes it unlikely that the stratigraphic trend at Guru Fatima resulted from mixing between a low $\delta^{98/95}$Mo endmember associated with Mn-oxide adsorption, and a high $\delta^{98/95}$Mo endmember associated with conversion of Mo to $MoO_xS_{4-x}^{2-}$ (e.g. Poulson et al., 2006; Neubert et al., 2008; Eriksson and Helz, 2000). Instead, two other scenarios could explain the

stratigraphic trend of $\delta^{98/95}$Mo: (i) An enhanced rate of Mo scavenging under the most reducing conditions indicated by the Fe-speciation data (between 0 and 1 m height), which moved sediment $\delta^{98/95}$Mo to compositions closer to ambient seawater (e.g. Poulson et al., 2006). (ii) A change in the speciation of $MoO_xS_{4-x}^{2-}$ as dissolved sulphide concentrations increased (e.g. Eriksson and Helz, 2000; Nägler et al., 2011), with different species having different fractionation factors from seawater. The samples with low $\delta^{98/95}$Mo above the CIE have very low [Mo] and are likely to reflect the composition of local detrital sources.

In contrast, $\delta^{98/95}$Mo values at Kheu River range from $-1.51\permil$ to $-0.36\permil$ even for samples where [Mo] is greater than the continental average of ~1.1 ppm (Rudnick and Gao, 2003). This range in isotopic composition is lower than the likely $\delta^{98/95}$Mo of Mo derived from the continents and lower than might be expected if Mo incorporation was due primarily to conversion to sulphide species (Archer and Vance, 2008; McManus et al., 2002; Poulson et al., 2006; Siebert et al., 2006). The Mo enrichments and Mn/Al ratios at Kheu River suggest that the environment during the PETM was anoxic, with a fluctuating redox-cline. The large enrichment of Mn at the top of the interval of Mo enrichment (Fig. 2) is a diagnostic indicator for such conditions; the Mn enrichment is likely to have formed from the upwards migration of Mn(II) following Mn(III) reduction, followed by reprecipitation at the redoxcline as Mn-oxide (Dickson et al., 2014). The $\delta^{98/95}$Mo data presented here can be explained by the incorporation of Mo into sediments by adsorption to Mn-oxides (with a fractionation of $\sim-3\permil$ from seawater), followed by reductive dissolution of Mn-oxides in sulphidic porewaters. This process would have released Mo back into solution, before its re-fixation as sulphides either deeper in the sediment column, or when bottom water sulphide concentrations became higher. It is difficult to distinguish between these scenarios, given that the depth of the Kheu River chemocline was likely to have fluctuated close to the sediment-water interface, and that bottom-waters were not also completely devoid of oxygen (Dickson et al., 2014). Likewise, Fe_{HR}/Fe_T data from the interval where [Mo] > 1 ppm fall in the range of 'possibly anoxic' conditions (0.22–0.38, Poulton and Canfield, 2011) indicating either that oxygen was present permanently at concentrations <10 µmol/l (Shaw et al., 1990), or that oxygen was delivered sporadically by bottom-water re-oxidation events.

5. The Mo-isotope signatures of continental margin sediments and seawater in the early Eocene

The $\delta^{98/95}$Mo values of present-day anoxic continental margin sediments from several locations display a near constant ΔMo of $\sim0.7\permil$ (e.g. McManus et al., 2002; Poulson et al., 2006; Poulson-Brucker et al., 2009). It was postulated (Poulson et al., 2006) that this signature records a natural isotope fractionation between MoO_4^{2-} in seawater and authigenic $MoO_xS_{4-x}^{2-}$. A recent laboratory experiment supports this view by showing that the formation of authigenic Mo-sulphides under high dissolved [Mo] are fractionated by $-0.9 \pm 0.2\permil$ compared to the host solution (Poulson-Brucker et al., 2012), which is similar to the $\sim0.7\permil$ fractionation observed in nature (McManus et al., 2002; Poulson et al., 2006; Poulson-Brucker et al., 2009). Importantly, at anoxic continental margin locations, the rate of Mo scavenging from the water column is unlikely to exceed the rate of MoO_4^{2-} replenishment from the open ocean, thereby preserving a seawater–sulphide fractionation in sediments that accumulate there. In contrast, where partially restricted hydrological conditions exist, the replenishment of MoO_4^{2-} could be appreciably slower than the rate of Mo removal into underlying sediments, thereby causing the sediment $\delta^{98/95}$Mo to move closer to that of seawater (Poulson et al., 2006).
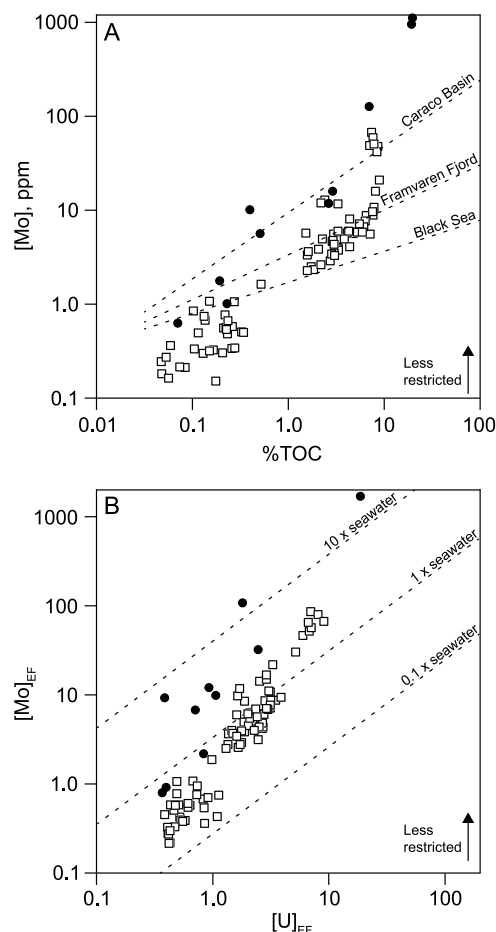

Fig. 3. A: Mo/TOC ratios from Kheu River (squares) and Guru Fatima (closed circles). Lines indicate the Mo/TOC gradients in present day marine environments: Black Sea (~4.5), Cariaco Basin (~9), Framvaren Fjord (~25) (Algeo and Lyons, 2006). B: [Mo] and [U] enrichment factors from Kheu River (squares) and Guru Fatima (closed circles). Dashed lines represent the $0.1\times$, $1\times$ and $10\times$ seawater Mo/U molar ratio (converted to sedimentary enrichments) of ~7.7.

The highest $\delta^{98/95}$Mo recorded at Guru Fatima is $0.96 \pm 0.05\permil$ ($n = 3$), which is, within uncertainty, $0.7\permil$ lower than a recent estimate of the seawater $\delta^{98/95}$Mo of $1.68 \pm 0.12\permil$ for the PETM recorded in the euxinic Arctic Basin (Dickson et al., 2012; Dickson and Cohen, 2012). The average $\delta^{98/95}$Mo for the entire anoxic CIE interval at Guru Fatima is $0.82 \pm 0.31\permil$, which is also, within uncertainty, $0.7\permil$ lower than the seawater $\delta^{98/95}$Mo. As discussed above, Mo incorporation into the Guru Fatima deposits by adsorption to Mn-oxides can be effectively ruled out due to their invariant Mn/Al ratio that parallels the typical continental crust value (Rudnick and Gao, 2003). Weakly sulphidic conditions, particularly at the base of the CIE, are supported by Fe_{PY}/Fe_{HR} ratios that only briefly cross the 0.7–0.8 threshold for local euxinia (Dickson et al., 2014). Indices of local seawater restriction (for example, Mo/U and Mo/TOC relationships (e.g. Algeo and Lyons, 2006; Algeo and Tribovillard, 2009)) do not show any evidence for hydrographic restriction at Guru Fatima across the study interval (Fig. 3), suggesting that it would be difficult for authigenic Mo deposition to deplete the overlying water column entirely of MoO_4^{2-}. Consequently, the $\delta^{98/95}$Mo recorded within the CIE are likely to reflect anoxic/weakly sulphidic porewater conditions at an open-ocean continental margin setting during the early Eocene, in a fashion analogous to the present-day sites studied by McManus et al. (2002), Siebert et al. (2006), Poulson et al. (2006) and Poulson-Brucker et al. (2009). The observation that these values are $\sim0.7\permil$ lower than coeval seawater (Dickson and

Cohen, 2012) is the first indication from the paleo-record to suggest that this offset reflects a fixed fractionation between MoO_4^{2-} and $MoO_xS_{4-x}^{2-}$ in anoxic and sulphidic porewaters (Poulson et al., 2006).

6. Implications

The results presented in this study show that the difference in $\delta^{98/95}Mo$ of $\sim 0.7\text{‰}$ between the Mo-isotope composition of present day anoxic continental margin sediments exposed to open-ocean hydrographic exchange and the Mo-isotope composition of seawater can also be found in the paleo-record. The results also suggest that accurate interpretation of $\delta^{98/95}Mo$ signatures from mudrocks requires supporting information not just on local redox conditions (e.g. Gordon et al., 2009) but also on the palaeoceanographic setting. Local environmental conditions will determine whether seawater MoO_4^{2-} can be drawn down quantitatively from seawater under highly sulphidic conditions, or whether sediments will record a sulphidic $\delta^{98/95}Mo$ signature that is offset from seawater due to rapid seawater renewal and non-quantitative Mo drawdown. The data from Guru Fatima are an example of this principle: in the absence of supporting information, the sample at the base of the CIE with $Fe_{PY}/Fe_{HR} > 0.8$ could be interpreted as recording the seawater $\delta^{98/95}Mo$. However, this interpretation would clearly be incorrect, given that (a) a much higher $\delta^{98/95}Mo$ was recorded in the Arctic Ocean for the same time interval, and (b) the Guru-Fatima site was exposed to rapid open ocean renewal of dissolved Mo, thus preventing the quantitative removal of Mo into the accumulating sediments, despite the locally sulphidic conditions. It is possible that by focusing primarily on the presence or absence of local euxinia as a criterion for determining whether $\delta^{98/95}Mo$ can be interpreted as a seawater value (e.g. Gordon et al., 2009), past studies may have overestimated the extent of seafloor anoxia by not placing sufficient emphasis on the role of paleoceanographic setting in governing the efficiency of Mo removal from seawater.

Acknowledgements

References

Algeo, T.J., Tribovillard, N., 2009. Environmental analysis of paleoceanographic systems based on molybdenum–uranium covariation. Chem. Geol. 268, 211–225.

Algeo, T.J., Lyons, T.W., 2006. Mo-total organic carbon covariation in modern anoxic marine environments: implications for analysis of paleoredox and paleohydrologic conditions. Paleoceanography 21, PA1016. http://dx.doi.org/10.1029/2004PA001112.

Archer, C., Vance, D., 2008. The isotopic signature of the global riverine molybdenum flux and anoxia in the ancient oceans. Nat. Geosci. 1, 597–600.

Arnold, G.L., Anbar, A.D., Barling, J., Lyons, T.W., 2004. Molybdenum isotope evidence for widespread anoxia in the mid-Proterozoic oceans. Science 304, 87–90.

Arnold, G.L., Lyons, T.W., Gordon, G.W., Anbar, A.D., 2012. Extreme changes in sulfide concentrations in the Black Sea during the Little Ice Age reconstructed using molybdenum isotopes. Geology 40, 595–598.

Barling, J., Anbar, A.D., 2004. Molybdenum isotope fractionation during adsorption by manganese oxides. Earth Planet. Sci. Lett. 217, 315–329.

Brennecka, G.A., Herrmann, A.D., Algeo, T.J., Anbar, A.D., 2011. Rapid expansion of oceanic anoxia immediately before the end-Permian mass extinction. Proc. Natl. Acad. Sci. USA 108, 17631–17634.

Canfield, D.E., 1989. Reactive iron in marine sediments. Geochim. Cosmochim. Acta 53, 619–632.

Crusius, J., Calvert, S., Pedersen, T., Sage, D., 1996. Rhenium and molybdenum enrichments in sediments as indicators of oxic, suboxic and sulphidic conditions of deposition. Earth Planet. Sci. Lett. 145, 65–78.

Dickson, A.J., Cohen, A.S., 2012. A molybdenum isotope record of Eocene Thermal Maximum 2: implications for global ocean redox during the early Eocene. Paleoceanography 27, PA3230. http://dx.doi.org/10.1029/2012PA002346.

Dickson, A.J., Cohen, A.S., Coe, A.L., 2012. Seawater oxygenation during the Paleocene–Eocene Thermal Maximum. Geology 40. http://dx.doi.org/10.1130/G32977.1.

Dickson, A.J., Rees-Owen, R.L., März, C., Coe, A.L., Cohen, A.S., Pancost, R.D., Taylor, K., Shcherbinina, E., 2014. The spread of marine anoxia on the Northern Tethys margin during the Paleocene–Eocene Thermal Maximum. Paleoceanography 29 (6), 471–488. http://dx.doi.org/10.1002/2014PA002629.

Duan, Y., Anbar, A.D., Arnold, G.L., Lyons, T.W., Gordon, G.W., Kendall, B., 2010. Molybdenum isotope evidence for mild environmental oxygenation before the Great Oxidation Event. Geochim. Cosmochim. Acta 74, 6655–6668.

Emerson, S.R., Huested, S.S., 1991. Ocean anoxia and the concentrations of molybdenum and vanadium in seawater. Mar. Chem. 34, 177–196.

Eriksson, B.E., Helz, G.R., 2000. Molybdenum (IV) speciation in sulphidic waters: stability and lability of thiomolybdates. Geochim. Cosmochim. Acta 64, 1149–1158.

Gavrilov, Y.O., Kodina, L.A., Lubchenko, I.Y., Muzylev, N.G., 1997. The late Paleocene anoxic event in epicontinental seas of Peri-Tethys and formation of the sapropelite unit: sedimentology and geochemistry. Lithol. Min. Res. 32, 427–450.

Gavrilov, Y.O., Muzylöv, N.G., 1992. The geochemistry of sapropelite interbeds in the Paleogene of Central Caucasus. Lithol. Min. Res. 26, 548–559.

Gavrilov, Y., Shcherbinina, E., Golovanova, O., Porovsky, B., 2009. A variety of PETM records in different settings, northeastern Peri-Tethys. In: Crouch, E.M., Strong, C.P., Hollis, C.J. (Eds.), Climatic and Biotic Events of the Paleogene (CBEP 2009), Extended Abstracts from an International Conference in Wellington, New Zealand. In: GNS Sci. Misc. Ser., vol. 18, pp. 67–70.

Goldberg, T., Archer, C., Vance, D., Poulton, S.W., 2009. Mo isotope fractionation during adsorption onto Fe (oxyhydr)oxides. Geochim. Cosmochim. Acta 73, 6502–6516.

Goldberg, T., Gordon, G., Izon, G., Archer, C., Pearce, C.R., McManus, J., Anbar, A.D., Rehkmper, M., 2013. Resolution of inter-laboratory discrepancies in Mo isotope data: an intercalibration. J. Anal. At. Spectrom. 28, 724–735. http://dx.doi.org/10.1039/c3ja30375f.

Gordon, G.W., Lyons, T.W., Arnold, G.L., Roe, J., Sageman, B.B., Anbar, A.D., 2009. When do black shales tell molybdenum isotope tales? Geology 37, 535–538.

Greber, N.D., Siebert, C., Ngler, T.F., Petke, T., 2012. $^{98/95}Mo$ values and molybdenum concentration data for NIST SRM 610, 612 and 3134: towards a common protocol for reporting Mo data. Geostand. Geoanal. Res. 36, 291–300.

Kendall, B., Gordon, G.W., Poulton, S.W., Anbar, A.D., 2011. Molybdenum isotope constraints on the extent of late Paleoproterozoic ocean euxinia. Earth Planet. Sci. Lett. 307, 450–460.

Lehmann, B., Nagler, T.F., Holland, H.D., Wille, M., Mao, J., Pan, J., Ma, D., Dulski, P., 2007. Highly metalliferous carbonaceous shale and Early Cambrian seawater. Geology 35, 403–406.

McManus, J., Nägler, T., Siebert, C., Wheat, C.G., Hammond, D.E., 2002. Oceanic molybdenum isotope fractionation: diagenesis and hydrothermal ridge-flank alteration. Geochem. Geophys. Geosyst. 1078. http://dx.doi.org/10.1029/2002GC0003569.

Montoya-Pino, C., Weyer, S., Anbar, A.D., Pross, J., Oschmann, W., van de Schootbrugge, B., Arz, H.W., 2010. Global enhancement of ocean anoxia during Oceanic Anoxic Event 2: a quantitative approach using U isotopes. Geology 38, 315–318.

Morford, J.L., Emerson, S., 1991. The geochemistry of redox sensitive trace metals in sediments. Geochim. Cosmochim. Acta 63 (11–12), 1735–1750.

Nägler, T.F., Neubert, N., Böttcher, M.E., Dellwig, O., Schnetger, B., 2011. Molybdenum isotope fractionation in pelagic euxinia: evidence from the modern Black and Baltic Seas. Chem. Geol. 289, 1–11.

Neubert, N., Nägler, T.F., Böttcher, M.E., 2008. Sulphidity controls molybdenum isotope fractionation into euxinic sediments: evidence from the modern Black Sea. Geology 36, 775–778.

Pancost, R.D., Crawford, N., Magness, S., Turner, A., Jenkyns, H.C., Maxwell, J.R., 2004. Further evidence for the development of photic-zone euxinic conditions during Mesozoic oceanic anoxic events. J. Geol. Soc. Lond. 161, 353–364.

Pearce, C.R., Cohen, A.S., Coe, A.L., Burton, K.W., 2008. Molybdenum isotope evidence for global ocean anoxia coupled with perturbations to the carbon cycle during the early Jurassic. Geology 36, 231–234.

Pearce, C.R., Cohen, A.S., Parkinson, I.J., 2009. Quantitative separation of molybdenum and rhenium from geological materials for isotopic determination by MC-ICP-MS. Geostand. Geoanal. Res. 33, 219–229.

Piper, D.Z., Calvert, S.E., 2009. A marine biogeochemical perspective on black shale deposition. Earth-Sci. Rev. 95, 63–96.

Poulson, R.L., Siebert, C., McManus, J., Berelson, W.M., 2006. Authigenic molybdenum isotope signatures in marine sediments. Geology 34, 617–620.

Poulson-Brucker, R.L., McManus, J., Severmann, S., Berelson, W.M., 2009. Molybdenum behaviour during early diagenesis: insights from Mo isotopes. Geochem. Geophys. Geosyst. 10, Q06010. http://dx.doi.org/10.1029/2008GC002180.

Poulson-Brucker, R.L., McManus, J., Poulton, S.W., 2012. Molybdenum isotope fractionations observed under anoxic experimental conditions. Geochem. J. 46, 201–209.

Poulton, S.W., Canfield, D.E., 2011. Ferruginous conditions: a dominant feature of the ocean through Earth's history. Elements 7 (2), 107–112.

Raiswell, R., Buckley, F., Berner, R.A., Anderson, T.F., 1988. Degree of pyritization as a paleoenvironmental indicator of bottom-water oxygenation. J. Sediment. Petrol. 58, 812–819.

Reitz, A., Wille, M., Nägler, T.F., de Lange, G.J., 2007. Atypical Mo isotope signatures in eastern Mediterranean sediments. Chem. Geol. 245, 1–8.

Rudnick, R.L., Gao, S., 2003. Composition of the continental crust. In: Heinrich, D.H., Karl, K.T. (Eds.), Treatise on Geochemistry. Pergamon, Oxford, UK, pp. 1–64.

Scheiderich, K., Zerkle, A.L., Helz, G.R., Farquhar, J., Walker, R.J., 2010. Molybdenum isotope, multiple sulfur isotope, and redox-sensitive element behavior in early Pleistocene Mediterranean sapropels. Chem. Geol. 279, 134–144.

Scott, C., Lyons, T.W., 2012. Contrasting molybdenum cycling and isotopic properties in euxinic versus non-euxinic sediments and sedimentary rocks: refining the paleoproxies. Chem. Geol. 324–325, 19–27.

Scott, C., Lyons, T.W., Bekker, A., Shen, Y., Poulton, S.W., Chu, X., Anbar, A.D., 2008. Tracing the stepwise oxygenation of the Proterozoic ocean. Nature 452, 456–459.

Shaw, T.J., Gieskes, J.M., Jahnke, R.J., 1990. Early diagenesis in differing depositional environments: the response of transition metals in pore water. Geochim. Cosmochim. Acta 54, 1233–1246.

Siebert, C., McManus, J., Bice, A., Poulson, R., Berelson, W.M., 2006. Molybdenum isotope signatures in continental margin sediments. Earth Planet. Sci. Lett. 241, 723–733.

Siebert, C., Nägler, T.F., von Blanckenburg, F., Kramers, J.D., 2003. Molybdenum isotope records as a potential new proxy for paleoceanography. Earth Planet. Sci. Lett. 211, 159–171.

Stirling, C., Anderson, M.B., Potter, E.-K., Halliday, A.N., 2007. Low-temperature isotopic fractionation of uranium. Earth Planet. Sci. Lett. 264, 208–225.

Summons, R.E., Powell, T.G., 1987. Identification of aryl isoprenoids in source rocks and crude oils: biological markers for the green sulphur bacteria. Geochim. Cosmochim. Acta 51 (3), 557–566.

Tossell, J.A., 2005. Calculating the partitioning of the isotopes of Mo between oxidic and sulfidic species in aqueous solution. Geochim. Cosmochim. Acta 69, 2981–2993.

Tribovillard, N., Algeo, T.J., Lyons, T., Riboulleau, A., 2006. Trace metals as paleoredox and paleoproductivity proxies: an update. Chem. Geol. 232, 12–32.

Wen, H., Zhang, Y., Fan, H., Hu, R., 2009. Mo isotopes in the lower Cambrian formation of southern China and its implications on paleo-ocean environment. Chin. Sci. Bull. 54, 4756–4762.

Weyer, S., Anbar, A.D., Gerdes, A., Gordon, G.W., Algeo, T.J., Boyle, E.A., 2008. Natural fractionation of $^{238}U/^{235}U$. Geochim. Cosmochim. Acta 72, 345–359.

Wille, M., Nägler, T.F., Lehmann, B., Schröder, D., Kramers, J.D., 2008. Hydrogen sulphide release to surface waters at the Precambrian/Cambrian boundary. Nature 435, 767–769.

Zhou, L., Wignall, P.B., Su, J., Feng, Q., Xie, S., Zhao, L., Huang, J., 2012. U/Mo and $^{98/95}$Mo as local and global redox proxies during mass extinction events. Chem. Geol. 324–325, 99–107.